A Study of Microwave Transmission, Reflection, Absorption, and Shielding Effectiveness of Conducting Polypyrrole Films

AKIF KAYNAK,[1,*] JOE UNSWORTH,[1] RAY CLOUT,[2] ANANDA S. MOHAN,[2] and GEOFFREY E. BEARD[2]

[1]University of Technology, Sydney, Centre for Materials Technology, School of Physical Sciences, and
[2]School of Electrical Engineering, P.O. Box 123, Broadway, NSW 2007, Sydney, Australia

SYNOPSIS

Microwave transmission, reflection, and absorption behavior and the shielding effectiveness of electrochemically synthesized polypyrrole films with dc conductivities ranging from 0.001 to 50 S/cm are presented. Results show that the electrical conductivity of the doped polypyrrole films has a significant effect on transmission, reflection, and absorption of microwaves. Heavily doped, conducting films were highly reflective, whereas lightly doped, semiconducting films had very high transmission. Intermediate conductivity polypyrrole samples were highly absorptive. The agreement between experimental data and theoretical modeling provided confidence to extend the modeling to include the effect of sample thickness on the transmission, reflection, and absorption properties of films with a wide range of conductivity values, hence, providing valuable information for the design of microwave devices and fundamental understanding of the material properties. A method of measuring the far-field shielding effectiveness of polypyrrole films is also presented. Results of shielding experiments indicated the potential for such applications. © 1994 John Wiley & Sons, Inc.

INTRODUCTION

Whether intrinsically conducting or in the composite form, conducting polymers have been a popular area of research and numerous articles on chemical, electrical, and mechanical properties have been published. Microwave properties, however have only recently become an area of research interest. There has been a few recent publications on the microwave dielectric properties[1-6] and absorption behavior of conducting polymers and composites. However, a comprehensive study of microwave transmission, reflection, and absorption properties of any intrinsically conducting polymer has not been done so far. Yet, reliable data on these properties would be indispensable for any attempt in using these materials in microwave device applications. This article is a detailed study of microwave transmission, reflection, and absorption behavior of polypyrrole films with electrical conductivities ranging from semiconducting to highly conducting with a view to potential microwave applications. The data presented in this article is directly related to the dielectric data of our previous publications,[4,7] as the transmission and reflection data presented here were verified by theoretical methods using the dielectric data and vice versa.

In a recent publication,[8] microwave absorbance of composites of polypyrrole dispersed in rubber and epoxy resin, blends of polypyrrole obtained by *in situ* chemical growth in an insulating phase such as Teflon, and blends of polyaniline and poly(3-octylthiophene) were discussed. The conductivity of the material was reduced to 10^{-3} to 10^{-1} S/cm by either reducing the doping level or blending with an insulating phase to produce an absorbing material. Blends of polypyrrole obtained by *in situ* chemical growth differed considerably from dispersion blends of polypyrrole. The former had an extremely low percolation boundary, hence, resulting in a material with the rheological properties of the insulating matrix and reproducible microwave properties; the dispersion blends, however, did not have stable property levels. When a comparison is made among the three conducting polymers, polypyrrole easily formed blends with the insulating polymers, whereas

* To whom correspondence should be addressed.

Journal of Applied Polymer Science, Vol. 54, 269-278 (1994)
 CCC 0021-8995/94/030269-10

polyaniline-based absorbents had the ability to be deposited onto reinforcing textiles and polyalkylthiophene had excellent solubility and melting properties that were more difficult with other conducting polymers. The wide range of conductivities obtained with conducting polymers allowed a fine control in the design of absorbing materials.

Microwave reflectivity and absorption of large-area conducting polypyrrole composites was investigated in the frequency range 2–18 GHz using a free-space reflectivity arch and a vector network analyzer.[9] Electrical properties of the polymer were controlled by adjusting the concentration of the pyrrole monomer. High monomer concentration produced films with low sheet resistivity and the microwave reflectivity was high and independent of frequency, whereas polypyrrole composite sheets with high resistivity had low microwave reflectivity and they showed a marked frequency dependence. Salisbury screen and Jaumann-type absorbers were constructed by sandwiching polystyrene foam spacers with polypyrrole composites.

The potential of iodine-doped poly-*p*-phenylene-benzopisthiazole (PBT) in microwave absorbers was also examined.[10] Double- and single-layer electric Salisbury screens using PBT were fabricated. Absorption of 90% was achieved with single-layer screens. The bandwidth of the absorber was found to increase from 2 to 7 GHz by constructing a multiple screen absorber.

In a further study, the effect of frequency, electrical thickness, doping, polarization, and angle of incidence on the plane wave shielding effectiveness of conducting polyacetylene and iodine-doped PBT were evaluated.[11] Single and multiple layers of conducting polymers were utilized and shielding effectiveness values exceeding 40 dB were recorded. Microwave conductivity of iodine-doped PBT films over a temperature range of 20–400 K were determined using the cavity perturbation technique. The measured conductivity values were used to evaluate the reflection and transmission of the polymer. Transmission data as a function of layer thickness, frequency, doping level, polarization, and angle of incidence indicate potential in high data-rate electronic equipment and for commercial aerospace applications.

EXPERIMENTAL

Synthesis of Polypyrrole

A galvanostatic electrochemical synthesis method was employed for the oxidative polymerization of polypyrrole.[12] A two-electrode cell was employed with polymerization occurring at a horizontally oriented stainless-steel type 304 anode. Stainless-steel gauze suspended above the anode was employed as the cathode. A pyrrole concentration of $0.2M$ in aqueous solution was used. Polypyrrole films of varying electrical conductivities were synthesized using a range of *p*-toluenesulfonate (*p*-TS) anion dopant concentrations. During the preparation of the supporting electrolyte, and prior to pyrrole addition, the pH of the solution was adjusted to approximately 11 to completely deprotonate the *p*-TS into the anion form. Synthesis was carried out at an optimum current density of 3.0 mA cm^{-2} over 30 min at 2°C to yield a film of the order of 50 microns in thickness. The electrolyte was stirred during synthesis to achieve uniform monomer concentration throughout.

Free-standing films were peeled from the anode using a scalpel and vacuum-dried. The films were stored at −10°C in the dark. The dc conductivity of the resulting film was determined using the standard four-probe method.

Microwave Transmission, Reflection, and Absorption Measurements

Polypyrrole films were sandwiched between two waveguides to coaxial transducers connected to a Hewlett-Packard Automatic Network Analyzer 8720A, calibrated in the transmission mode to obtain reflection and transmission coefficients (Fig. 1). Since each sample was larger than the waveguide opening, the problem of losses at corners and edges was eliminated. Consequently, accurate and reproducible reflection and transmission measurements were achieved.

Both the insertion loss (transmission coefficient) and return loss (reflection coefficient) were directly read in decibels (dB). A signal reflected from the sample is measured as a ratio and expressed as

$$\text{Reflection coefficient} = \text{reflected/incident} = \Gamma = \rho < \varphi$$

$$\text{Return loss (dB)} = -20 \log \rho.$$

The reflection coefficient $\rho = 1$ indicates that all of the incident signal is reflected back at port 1, whereas the reflection coefficient $\rho = 0$ indicates that none of the signal is reflected.

Accuracy of network analyzer measurements is dependent on an accurate calibration. Parts of the experimental setup such as cable adaptors and the

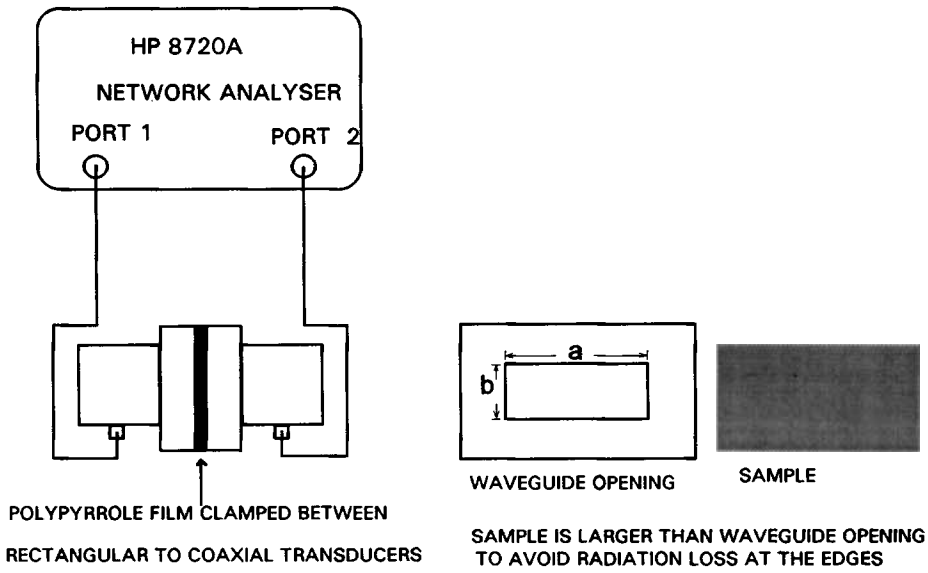

Figure 1 Microwave transmission and reflection measurements at 10 and 2.45 GHz using rectangular to coaxial transducers.

instrument itself all introduce variations in magnitude and phase of the signal, masking the actual properties of the material under test. The calibration removes the effects of repeatable measurement variations in the experimental setup. Before calibration is performed, the appropriate frequency and the bandwidth are selected. A two-port measurement calibration is then performed using precision standards such as short, matched load and a matched transmission line. The two-port method is the most accurate calibration for transmission and reflection measurements as it measures the systematic errors due to frequency response, leakage, and mismatch in both forward and reverse directions and removes their effects from the measurements.

The network analyzer measures the magnitude and the phase of the reflected power from the sample and power transmitted through the sample with respect to the incident wave. The amplitude and phase are expressed as scattering parameters, s_{11} and s_{21}, from which percent reflection and transmission values and real and imaginary parts of the complex dielectric constant can be calculated. The analysis was carried out at frequencies of 2.45 and 10 GHz with a span of 0.1 GHz.

Shielding Effectiveness Measurements on Polypyrrole Films

The shielding effectiveness of a material is defined as the ratio of transmitted power to incident power at a given frequency. Shielding effectiveness of a material for plane wave radiation is an important characteristic that quantifies the ability of the material under test to shield against radiation from electromagnetic sources that are located at distances greater than at least a wavelength away from the source of the radiation.[13] To measure the electromagnetic shielding effectiveness of a thin conductive film for the plane wave condition, it is necessary to interpose the test material between a source of plane waves and an appropriate detector. Hence, it is important to design a structure that can support waves similar to plane waves. A uniform plane wave is a special case of a transverse electromagnetic (TEM) wave. A TEM wave does not contain any components of electric or magnetic fields in the direction of wave propagation. Hence, the plane wave testing can be done in a waveguiding structure that can support a TEM mode. Conventional hollow rectangular or circular waveguides cannot support TEM modes and, hence, are not used for measuring the plane wave shielding effectiveness. Coaxial structures containing circular inner and outer conductors have been used for measuring shielding effectiveness.[14] The accuracy obtained using this method is very sensitive to the precise location of the sample in the coaxial line, as the presence of any air gaps between the toroid-shaped sample and the coaxial line may give rise to inaccurate readings. In addition, the problem of contact resistance would also limit the accuracy of this method. To circumvent these problems, a new measurement technique based on the TEM cell has been proposed.[15,16] A new TEM

test cell was designed and fabricated for measuring the shielding effectiveness of the polypyrrole samples.

A TEM cell is basically a rectangular coaxial line tapered at each end so as to adapt to standard coaxial connectors. TEM cells are extensively used for measuring electromagnetic emission and susceptibility testing of electronic equipment.[17] The TEM cell has rectangular inner and outer conductors separated by a gap. A schematic view of the TEM cell arrangement for measuring the far-field shielding effectiveness is shown in Figure 2. The test arrangement consists of two halves of the TEM cell with an interrupted inner conductor of a rectangular cross section. The cell was designed for a characteristic impedance of 50 Ω. The gradual taper at each end of the cell was designed to minimize reflections. The rectangular cross section of the cell offers an advantage over a standard coaxial structure since the sample preparation and testing are nondestructive. Further, the problems of measurements arising due to air gaps is also avoided. Before shielding measurements are done, the network analyzer is calibrated using the full two-port calibration. The sample is then held between the two halves of the TEM cell. It is ensured that the sample completely covers the flanges and there is no direct contact between the two halves of the cell. Shielding measurements are carried out using the vector network analyzer. Initial measurements were done at 1 GHz, as the studies at this frequency is of practical importance in shielding design.

THEORY

For samples with relatively high electrical conductivity, the following transmission measurement model is used. In this model, large reflection coefficients are expected between the loaded and unloaded transmission line and within the loaded region of the line a large level of attenuation will take place. In such a model, multiple reflections are neglected and measurements are analyzed as a single-pass model.

The normalized characteristic impedance z in a

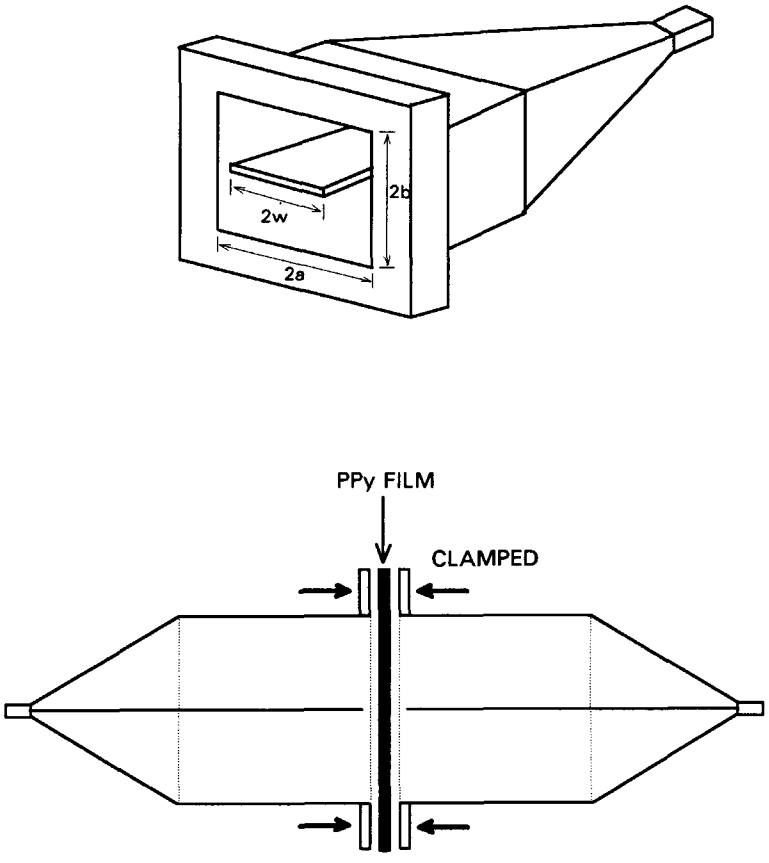

Figure 2 (a) One-half of the TEM cell. (b) TEM cell for measuring far-field shielding effectiveness.

line loaded with a lossy dielectric (Fig. 3) where the series resistive component is much less than the shunt conductive component is given by

$$z = \frac{1}{\sqrt{\varepsilon' - j\left(\varepsilon'' + \frac{\sigma}{\omega\varepsilon_0}\right)}} \tag{12}$$

The complex propagation constant γ for a lossy transmission line where the series-resistive component is much less than the conductive loss component can be derived as

$$\gamma = \alpha + \beta j = \beta_0\left[-\varepsilon' + j\left(\varepsilon'' + \frac{\sigma}{\omega\varepsilon_0}\right)\right]^{1/2} \tag{13}$$

where α and β are the propagation and phase constants, respectively.

The reflection coefficient when the incident radiation impinges on the sample at $y = 0$ (Fig. 3) is

$$\Gamma(0) = \frac{z-1}{z+1} = \frac{1 - \sqrt{\varepsilon' - j\left(\varepsilon'' + \frac{\sigma}{\omega\varepsilon_0}\right)}}{1 + \sqrt{\varepsilon' - j\left(\varepsilon'' + \frac{\sigma}{\omega\varepsilon_0}\right)}} \tag{14}$$

The more important reference plane for transmission measurements is the plane at $y = 0$. The transmission coefficient at the same plane is given by $1 + \Gamma(0)$. The rate of attenuation of the signal within the material is determined by the attenuation constant α.

Reflection and Transmission Calculations on a Highly Conducting Polypyrrole Film

To use eqs. (13) and (14), the sample conductivity σ and real and imaginary parts of the complex dielectric constant (ε' and ε'') are required. σ was measured by the standard four-probe technique as described in ASTM D4496-87. Complex dielectric constant measurements were done using a waveguide, the HP 8720A Vector Network Analyzer, and the HP 85071 Materials Measurement Software. The software activates the measurement of all four S parameters (S11, S21, S12, and S22) of the sample by controlling the network analyzer and using S parameters and sample thickness to calculate the complex permittivity.

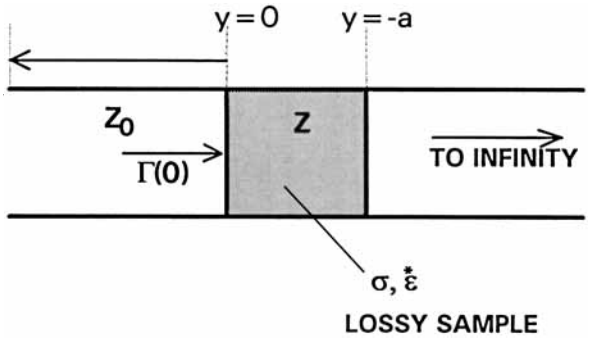

Figure 3 Sample in a transmission line.

Consider a polypyrrole film with a dc conductivity of $\sigma = 50$ S/cm = 5000 S/m. At 10 GHz, for the above sample, a good conductor condition, $[\sigma/(\omega\varepsilon_0)] \gg \varepsilon''$, is satisfied. Since the $\sigma/(\omega\varepsilon_0)$ term dominates, the propagation constant can be expressed as

$$\gamma = \alpha + i\beta = \beta_0\sqrt{j\frac{\sigma}{\omega\varepsilon_0}}$$

where $\beta_0 = \omega/c = (2\pi f)/c = 209.44$ rad/m. The calculations yield

$$\gamma = 14043.26 + j14043.26$$

where the attenuation constant $\alpha = 14043.26$ nepers/m.

The reflection coefficient is calculated and expressed in polar form:

$$\Gamma(0) = 0.9852 \angle 179.15°$$

expressing in decibels,

$$dB = 20 \log \frac{V_1}{V_2} = -0.1295 dB$$

97.062% at the sample plane. The transmission coefficient at the sample plane,

$$T = 1 + \Gamma(0) = 0.0208 \angle 44.650°$$

corresponds to a signal reduction of 33.64 dB from that incident on the interface at sample plane. The corresponding percent transmission value is 0.04325% of the incident radiation, which is in good agreement with the experimental transmission that resulted in a signal reduction of 32.8 dB from that of incident on the sample. The shielding effectiveness can be calculated from the above data by evaluating the ratio of transmitted to incident fields.

Skin Depth

The skin depth is defined as the depth in the material at which the level of the signal transmitted has fallen to a fraction $1/e$ of its value at $y = 0$, i.e.,

$$Ae^{-\alpha\delta} = \frac{A}{e} = Ae^{-1} \quad \text{or} \quad \delta = \frac{1}{\alpha}$$

With α calculated above at 14043.26 nepers/m, the skin depth evaluates to $\delta = \alpha^{-1} = (1/14043.26)$ m = 71.2 microns.

Computer Modeling

By using the Hewlett-Packard 85180A High-Frequency Structure Simulator (HFSS) software package, reflection and transmission properties of polypyrrole films were verified using the dielectric results obtained by the cavity perturbation methods. HFSS uses a simulation technique to analyze the electrodynamic behavior of three-dimensional passive structures by computing the scattering parameter (S parameter) response and electromagnetic field distribution. The waveguide interior is divided into hundreds of tetrahedral elements and the field in each region is obtained by numerically solving the Helmholtz equation. It is assumed that each port of the structure is excited with a wave traveling along an infinite waveguide having the same cross section as that of the ports. HFSS computes the full electromagnetic field pattern inside the waveguide structure and the S matrix from which magnitude of microwave transmission and reflection are calculated. The scattering matrix describes the ratio of signals transmitted or reflected in magnitude and phase at each port of the waveguide structure for a given incident field excitation.

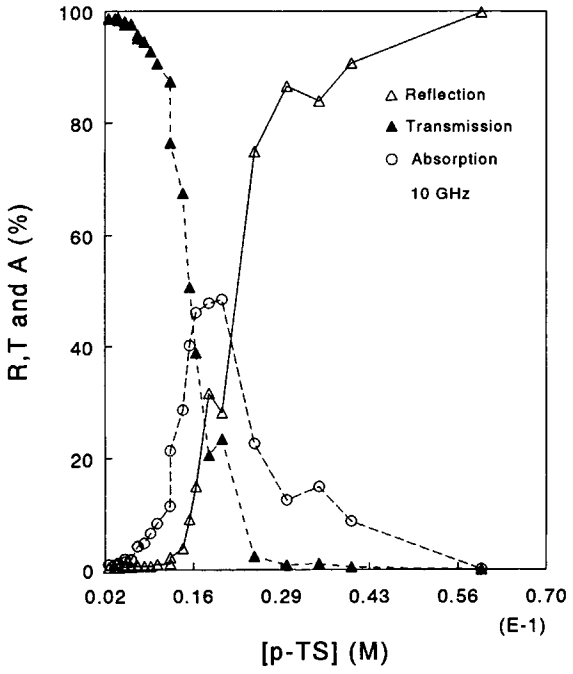

Figure 4 Experimental reflection, transmission, and absorption of polypyrrole films as a function of dopant concentration at 10 GHz.

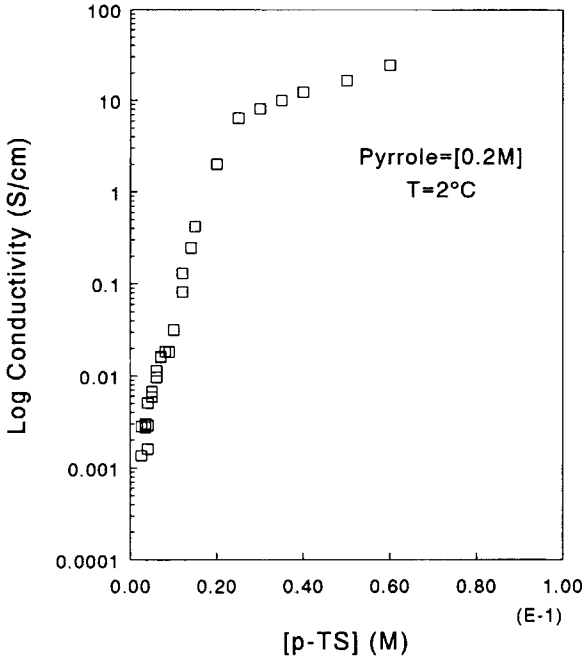

Figure 5 Dc conductivity of polypyrrole films vs. dopant concentration.

RESULTS AND DISCUSSION

Microwave reflection, transmission, and absorption of polypyrrole films at 10 GHz as a function of dopant concentration is presented in Figure 4. The corresponding electrical conductivity can be determined by referring to Figure 5. The results obtained at 2.45 GHz were found to be similar to the 10 GHz results.[4]

At very low electrical conductivities of polypyrrole, in the order of 10^{-3} S cm^{-1}, transmission of microwave radiation through the film is very high with very little reflection (low dielectric loss). At such low doping levels, there is very little interaction of the microwaves with the material. Conversely, at

high electrical conductivities (10–50 S cm^{-1}), microwave reflection is very high with almost no transmission (high dielectric loss). For example, a 44 micron-thick polypyrrole film with a dopant concentration of 0.060 *M* pTSA and a dc conductivity of 23 S/cm caused a signal reduction of 30.421 dB from that of impinging on the polymer surface, corresponding to a transmission of 0.09076% of the incident radiation at 10 GHz. At high doping levels, polypyrrole behaves like a metal with the collapse of the electric-field component of the microwave radiation occurring when it impinges on the high-conductivity film. However, at intermediate doping levels where there is maximum rate of change in reflection and transmission, a maximum in microwave absorption was observed at both 10 and 2.45 GHz. This peak in absorption suggests that the microwave radiation causes excitation of charge carriers at relatively low doping levels.

Transmission and reflection experiments conducted on polypyrrole films with various conductivities and thicknesses using rectangular to coaxial transducers at 10 GHz were modeled using HFSS. Since the thickness of polypyrrole films was about 50 microns, initial modeling was done on a 50 micron film. The agreement between the theoretical and experimental results can be seen by comparing Figures 4 and 6. In both graphs, maximum absorption corresponds to the maximum rate of change of transmission and absorption and maximum takes

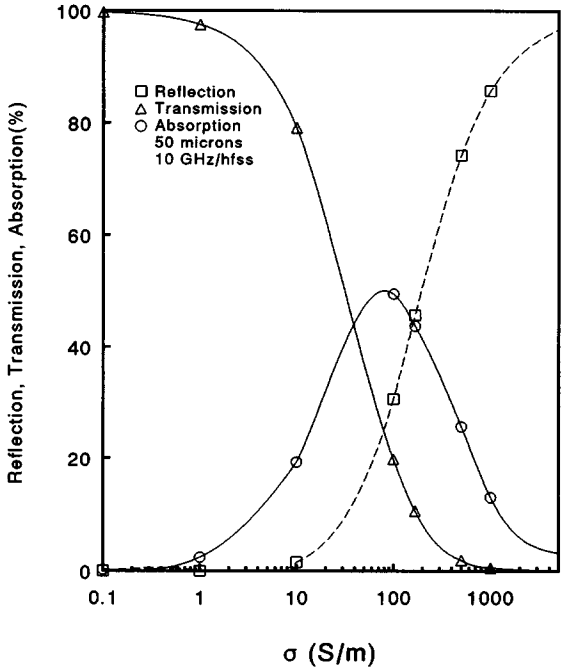

Figure 6 Theoretical reflection, transmission, and absorption vs. conductivity of 50 micron-thick films at 10 GHz, modeled at HFSS.

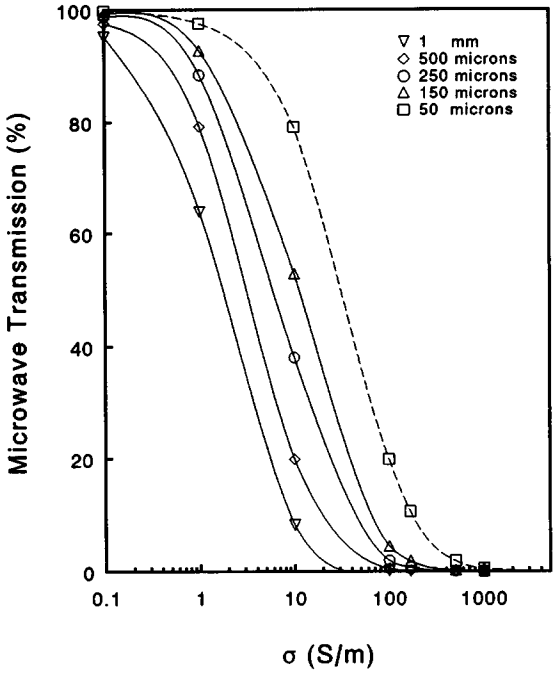

Figure 7 Transmission vs. conductivity of films with thicknesses ranging from 50 microns to 1 mm at 10 GHz, modeled at HFSS.

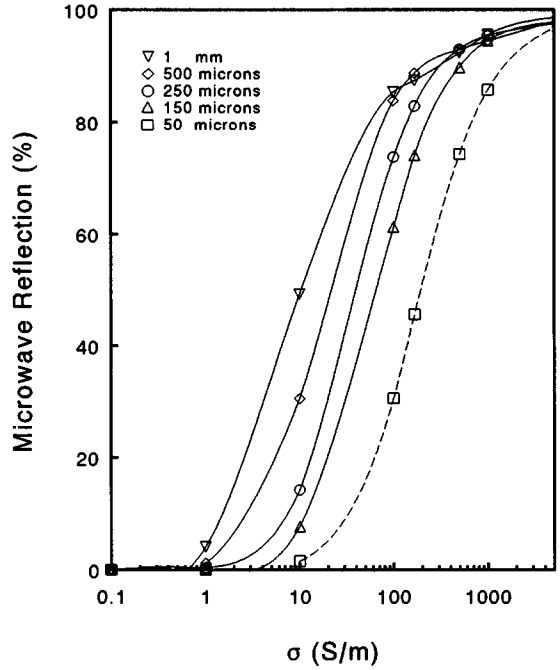

Figure 8 Reflection vs. conductivity at 10 GHz, modeled at HFSS.

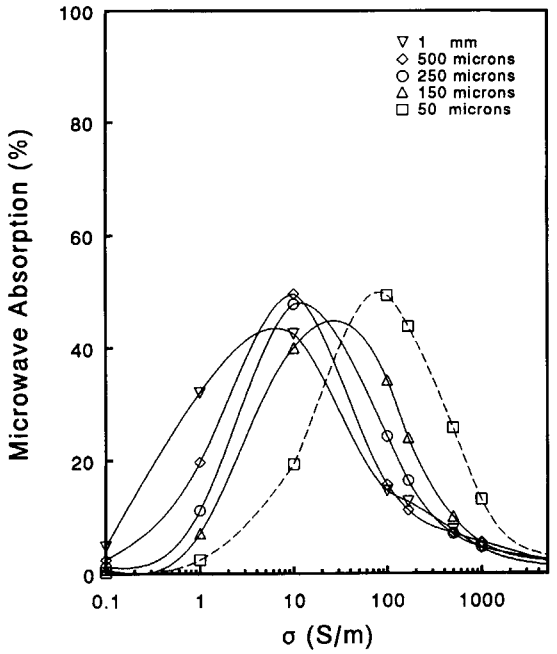

Figure 9 Absorption vs. conductivity at 10 GHz, modeled at HFSS.

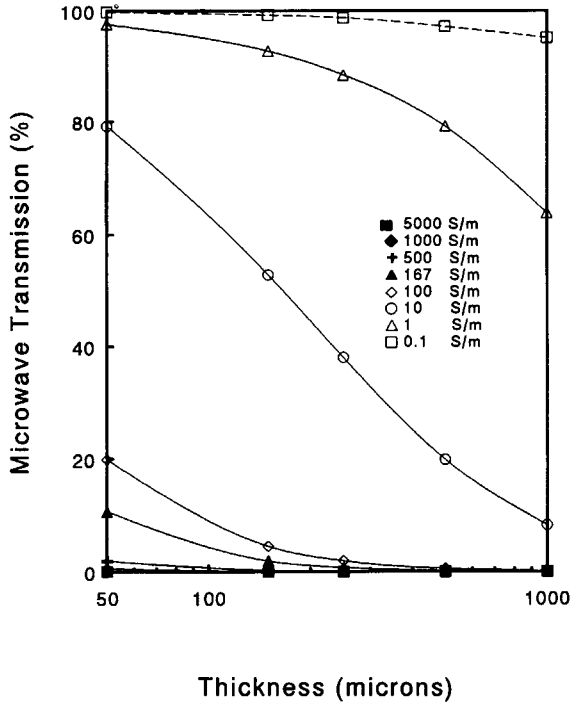

Figure 10 Theoretical transmission of films with conductivities ranging from 0.1 to 5000 S/m as a function of film thickness at 10 GHz, modeled at HFSS.

place at a conductivity of 1 S/cm for 50 micron films in both theory and experiment. Such an agreement between experiment and the model provided confidence to extend the modeling to include films with conductivities ranging from 10^{-3} to 50 S/cm and thicknesses ranging from 50 to 1000 microns.

When transmission, reflection, and absorption curves are grouped together and plotted as a function of conductivity, a rapid reflection increase and a rapid transmission decrease are observed (see Figs. 7–9). For thicker films, the changes took place at lower conductivities. The absorption peak shifted to higher conductivities with increase in thickness, i.e., for the 50 micron film, the absorption peak can be seen at 1 S/cm, whereas for the 1 mm film, the absorption peak is seen at about 0.007 S/cm.

When the reflection, transmission, and absorption data are expressed as a function of film thickness, the increase in the reflection and decrease in the transmission with the increase in film thickness can be seen (Figs. 10 and 11). Examination of the absorption–thickness curves reveals that heavily doped, highly conducting, and lightly doped semiconducting films were not absorptive in the given thickness range, whereas intermediate conductivity films exhibited maxima in absorption at different thicknesses depending on their doping levels (Fig. 12).

Reflection, transmission, and absorption exper-

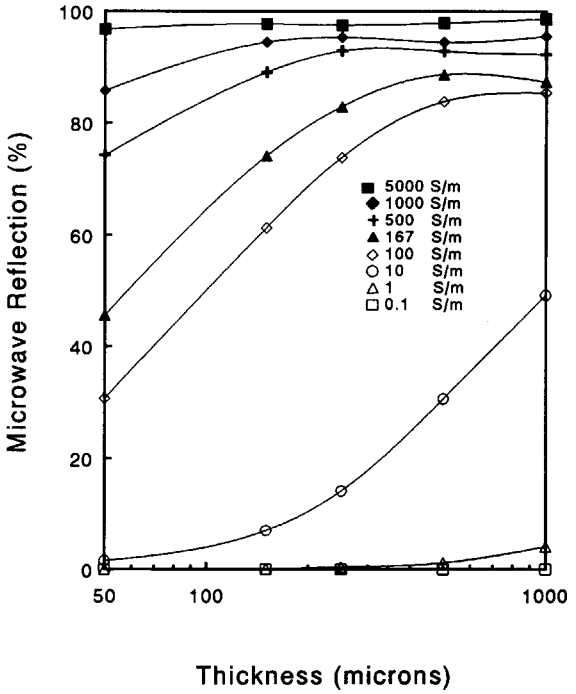

Figure 11 Reflection vs. thickness at 10 GHz, modeled at HFSS.

iments were done by placing the samples in rectangular waveguides that support the dominant TE_{10} modes. However, to simulate a real-life situation, TEM cells were designed and fabricated.

Initial far-field shielding effectiveness results at 1 GHz showed that shielding effectiveness increases with the conductivity of the shield (Fig. 13). Lightly doped, semiconducting polypyrrole had a negligibly low shielding effectiveness value, whereas a significant far-field shielding effectiveness of 38 dB was achieved with the highly doped, conductive sample.

CONCLUSION

Experiments described thus far have been aimed at characterizing polypyrrole in the microwave region. In this context, numerous experiments were conducted such as polymer synthesis, dc conductivity measurements, complex dielectric constant measurements,[4] and microwave transmission, reflection, and absorption measurements. Accuracy of the results were ensured by employing numerous measurement techniques, by testing standard materials, and by theoretical calculations.

Having access to such a system of tailoring transmission, reflection, absorption, and dielectric properties of polypyrrole in the microwave frequency region, combined with the stability of mechanical and electrical properties of the material, indicated the potential for novel microwave applications such as electromagnetic shields and radar absorbers. Presentation of microwave data in the form of charts of reflection, transmission, and absorption as functions of both conductivity and thickness will provide a valuable guide in achieving this aim. Further investigations into the far-field and near-field shielding effectiveness of intrinsically conducting polymers and composites are currently being undertaken. The results will be reported in future.

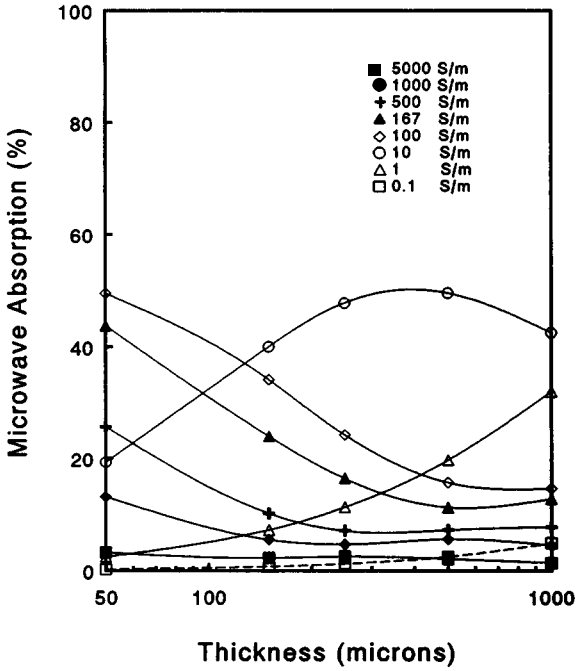

Figure 12 Absorption vs. thickness at 10 GHz, modeled at HFSS.

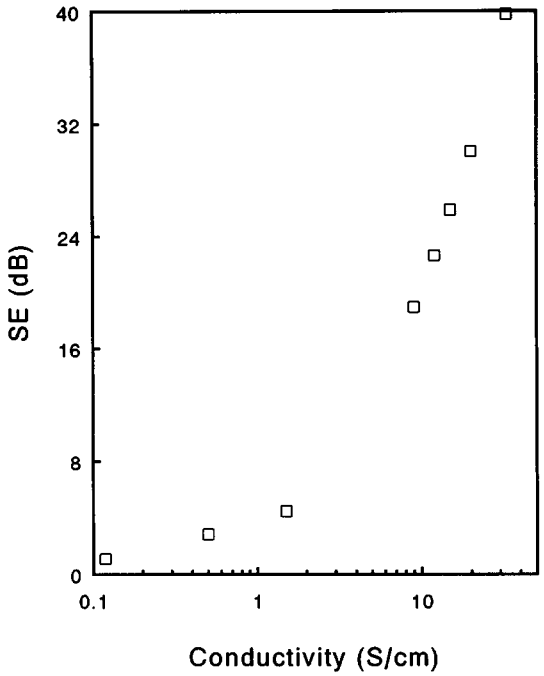

Figure 13 Far-field shielding effectiveness vs. conductivity at 1 GHz, measured in the TEM cell.

The authors would like to thank Professor W. R. Belcher and Dr. Rohana Ediriweera for their interest in the present work and for useful discussions.

REFERENCES

1. G. Phillips, R. Suresh, J. Chen, J. Waldman, J. Kumar, S. Tripathy, and J. Huang, *Solid State Commun.*, **76**(7), 963–966 (1990).
2. J. Unsworth, A. Kaynak, B. A. Lunn, and G. E. Beard, *J. Mater. Sci.*, **28**(12), 3307–3312 (1993).
3. F. Legros and A. F. Lamer, *Mater. Res. Bull.*, **19**(8), 1109–1117 (1984).

4. F. Epron, F. Henry, and O. Sagnes, *Makromol. Chem. Makromol. Symp.* **35/36,** 527–533 (1990).
5. K. Sato, M. Yamaura, T. Hagiwara, K. Murata, and Tokumoto, *Synth. Met.,* **40,** 35–48 (1991).
6. J. Ulanski, D. T. Glatzhofer, M. Przybylski, F. Kremer, A. Gleitz, and G. Wegner, *Polymer,* **28,** 859 (1987).
7. A. Kaynak, J. Unsworth, R. Clout, and G. E. Beard, *Mater. Res. Bull.,* to appear.
8. L. Olmedo, P. Hourquebie, and F. Jousse, *Adv. Mater.,* **5**(5), 373–377 (1993).
9. P. T. C. Wong, B. Chambers, A. P. Anderson, and P. V. Wright, *Elect. Lett.,* **28**(17), 1651–1653 (1992).
10. C. Chen and K. Naishadam, *IEEE Proceed.*-Southeastcom, **38** (1990).
11. K. Naishadam and P. K. Kadaba, *IEEE Trans. Microwave Theory Tech.,* **39**(7), 1158–1164 (1991).
12. D. S. Maddison and J. Unsworth, *Synth. Met.,* **30**(47) (1989).
13. H. W. Ott, *Noise Reduction Techniques in Electronic Systems,* Wiley, New York, 1976.
14. D. White and M. Mardiguian, *Shielding Materials,* Vol. 3, Series on EMC, ICT, Gainesville, FL, 1988.
15. M. L. Crawford, *IEEE Trans. Electromagn. Compat.,* **EMC-16**(4), 189–195 (1974).
16. J. Catrysse, in *Proceedings of 7th International Conference on Electromagnetic Compatibility,* York, England, 1990, pp. 62–67.

Received September 14, 1993
Accepted April 8, 1994